Ablation test-case series #3

- Numerical simulation of ablative-material response: code and model comparisons -

Tom van Eekelen * Alexandre Martin † Jean Lachaud ‡ Ioana Cozmuta §

I. Introduction

Code developers and users are curious to see "how their code compares" and "what are the effects of the different hypotheses in the models implemented". In 2011, an effort was started to allow such comparisons for ablative material response codes and models, in an open forum. Since then, each year, a test-case series has been proposed within the framework of the NASA/AFOSR/SNL ablation workshop - around February, each year. This year, it is targeted to release the final version of the test-case in the timeframe of the 6^{th} *Ablation Workshop* at the University of Illinois (10-11 April 2014). The test-case series are designed to propose problems of increasing complexity. Each series tackles only a few aspects of the material response to allow a targeted comparison of the codes and of the models. The first test-case was mostly a heat transfer problem chosen for it's simplicity, allowing to set the focus on the in-depth material response (it is summarized in section I.A). The second test-case series went one step further and made use of a convective boundary condition - as in state-of-the-art design codes and reached the state-of-the-art (see section I.B). This document presents the third series. The main goal of this new series, is to test the 2D-axisymmetrical and 3D modeling capabilities of the participating codes and assess multidimensional effects. All tests within test-case series #3 re-use the TACOT material properties (but with an extended pressure and B'_g range) defined for the previous series.[2]

I.A. Summary of the first test-case

The first test case was defined for the 4^{th} *Ablation Workshop, 1-3 March 2011, Albuquerque, New Mexico*.[1] It is a one-dimensional test-case focusing on the in-depth material response - fixed surface temperature and no recession. Three types of material-response codes have been identified during this first comparison:

- Type 1: based on the CMA[4] model or any mathematically equivalent model (heat transfer, pyrolysis, simplified mass transport);
- Type 2: CMA-type + Averaged momentum equation for the transport of the pyrolysis gases;
- Type 3: Higher fidelity codes (chemical/thermal non-equilibrium, etc).

The results had been provided by the participants before the workshop and a summary was presented during the workshop.[3] For type 1 and type 2 codes, differences in the temperature prediction were mostly below 1%. Type-3 code results were more scattered but they were mostly based on heuristic models that will need further validation.

I.B. Summary of the second test-case series

The definition of the test case series #2 was finalized in January 2012.[2] The second test-case series aims at reaching the state-of-the-art TPS-design level. For consistency with test-case series #1 and to limit time-investment, most of the parameters and boundary conditions are unchanged. The main modifications are: (1) convective boundary condition (instead of fixed surface-temperature boundary condition), and (2) surface recession is allowed. Computing the ablation rate to obtain the amount of surface recession is a

*Tom.vanEekelen@lmsintl.com
†Alexandre.Martin@uky.edu
‡jlachaud@ucsc.edu
§Ioana.Cozmuta@nasa.gov

complicated and still open problem. A traditional B' table is provided to facilitate the in-depth material-response comparison but other tables/methods may be used. A specific test-case dedicated to the estimation of the ablation rate is also proposed. Therefore, the test-case series #2 includes three traditional ablation tests and one additional test dedicated to the estimation of the ablation rate:

- 2.1: low heating, no recession (targeted surface temperature of about 1644 K, cf. test-case 1) - non-physical intermediate case without recession in preparation for 2.2.
- 2.2: low heating (same as test case 2.1), recession
- 2.3: high heating, recession (targeted surface temperature of about 3000 K)
- 2.4: computation of the ablation rate of TACOT for a temperature range of 300K-4000K and an air pressure of 101325 Pa (1 atm). This is often referred to as 'B' table'.

Participants compared their results at the 5^{th} *Ablation Workshop, Lexington, Kentucky, Feb 28-March 1, 2013*. Results of type-1 and type-2 codes were in overall satisfactory agreement, with several codes (at least 5) featuring perfectly matching results for cases 2.1, 2.2 and 2.3. For case 2.4, slight differences have been seen: nothing that may be alarming for design purpose, but the community agreed that the results are significantly affected by the thermodynamics data used - and somehow by the algorithm used. A more refined and dedicated test-case may be needed in the future.

II. Description of the third test-case series

A preliminary version of the test cases of series #3 has been presented at the 5^{th} *Ablation Workshop, Feb. 28- March 1, 2012*. Since then some modifications have been made; for example, a test case concerning a small re-entry vehicle[5] has been removed. The selected test-cases consist of an "Iso-Q" sample submitted to typical arc-jet conditions .[6,7] A total of four tests - with an increasing level of multidimensionality - are proposed:

- 3.0: a 2D-axisymmetric model with an isotropic version of TACOT without ablation. This test is a non-physical test only meant to help code developers calibrate their codes before going into the model/code comparison. Results for all type-2 codes are expected to be identical.
- 3.1: the same test but including ablation - and therefore, recession.
- 3.2: the same test but with an orthotropic version of TACOT, aligned with the "Iso-Q" sample axis.
- 3.3: a full 3D model with an orthotropic version of TACOT, tilted by 30° compared to the "Iso-Q" sample axis.

III. The "Iso-Q" test-case; geometry and boundary conditions

The "Iso-Q" sample geometry and the boundary conditions are described in this section. The so-called "Iso-Q" samples, used in arc-jet test, unfortunately do not display a fully iso-flux contour.[8] This is particularly true for sphere-cylinder geometries often used for testing.[8] They display a strong heat flux augmentation at the shoulder. In this test-case series, we wish to run uncoupled material-CFD simulations. It is therefore critical to use an initial shape with a more aero-thermodynamical profile, featuring a minimal heat flux augmentation at the shoulder. The idea is that even when running uncoupled simulations, the initial shape of the sample - and therefore the heat flux profile - should be conserved over time; that is, the ablation should be almost constant over most of the sample surface. A the same time, the initial geometry should be simple enough to ease the mesh generation - as participants do not necessarily have a lot of time to run the test-case series. Ellipse-cylinder geometries are good candidates as they allow the definition of continuous curvatures and are simple to define.

III.A. Geometry of the "Iso-Q" ellipse-cylinder sample

Current "Iso-Q" sphere-cylinder samples are often chosen with a sphere curvature radius equal to the diameter of the cylinder, as shown in figure 1. It was decided to use an ellipsoid instead of a sphere with a geometry as

close as possible to state-of-the-art samples. In other words, a 2D axisymmetrical projection, where the circle-arc and the small (D/16) shoulder radius will be replaced by a single ellipse arc, as shown in figure 2. The geometry of the modified "Iso-Q" specimen is then an ellipse on top of a cylinder. The cylinder has a radius of $R_{cyl} = 50$ mm, and the ellipse a major axis of $R_e = 50$ mm and a minor axis of $r_e = R(2 - \sqrt{3}) = 13.397$ mm. The dimensions are reproduced in Figure 2.

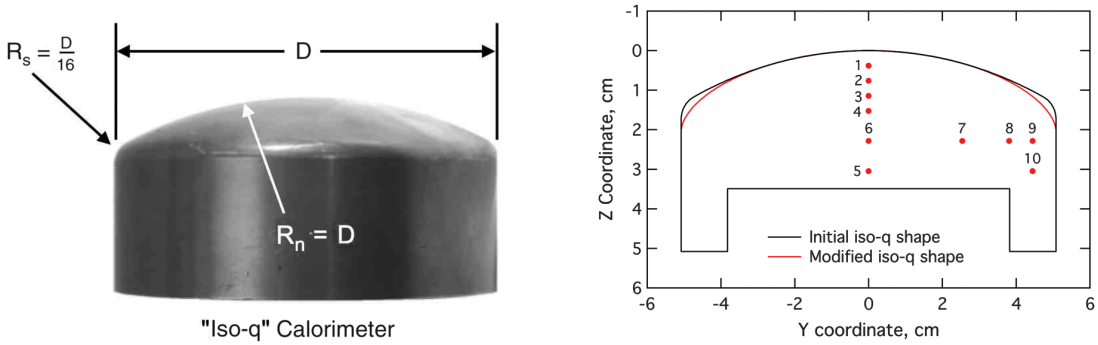

(a) "Iso-Q" test specimen

(b) position of the thermo-couples

Figure 1. State-of-the-art sample geometry and thermocouple placement.[6–8] NOTE: thermocouple placement is re-used but the geometry is slightly modified for the test-case series (see figure 2)

In Figure 1(b) and Table 1 we see the position of the thermo-couples, for which the temperature evolutions will be post-processed.

Table 1. Coordinates of the thermo-couples.

TC	Y-coordinate [cm]	Z-coordinate [cm]	TC	Y-coordinate [cm]	Z-coordinate [cm]
1	0.00	0.381	6	0.00	2.286
2	0.00	0.762	7	2.540	2.286
3	0.00	1.143	8	3.810	2.286
4	0.00	1.524	9	4.445	2.286
5	0.00	3.048	10	4.445	3.048

All the thermocouples are placed in the sample plane (x=0). This might not be ideal practice for a real sample but, here, it will greatly simplify the response post-processing for test 3.3.

"Iso-Q" test specimens include a support structure added to the geometry shown in Figure 1(b). Although the support structure will in general be made of a different material, here we will assume it is also made of TACOT for the simplicity of the analysis. Also, the contact between the "Iso-Q" sample and the support structure is assumed to be perfect. In other words, the example can be treated as a single block of TACOT. It is therefore allowed to create one continuous mesh/discretization for the "Iso-Q" and the support structure.

Please contact us if you find the definition unclear on incomplete. We will be happy to update the document accordingly.

III.B. Boundary conditions

The test-specimen is subjected to a similar heat load as applied in test 2.3 of test-case series #2. The specimen is subjected to a convective boundary condition. The sample is heated for 40 seconds, and it is let to cool-down for 1 minute by radiation cooling. The initial conditions are a uniform pressure and temperature: $p_0 = 0.004$ atm. (405.3 Pa), $T_0 = 300$ K. The initial gas composition in the material is left open. For type 1 and 2 codes, pyrolysis gas in thermal equilibrium is the usual practice. For type 3 codes, it is suggested to start with air. The time-dependent boundary-layer properties at the stagnation point are summarized in table 2. The other boundary-layer assumptions/properties are as follows for the code comparison:

- The factor for the blowing-correction correlation, used in the CMA model, is taken as $\lambda = 0.5$.

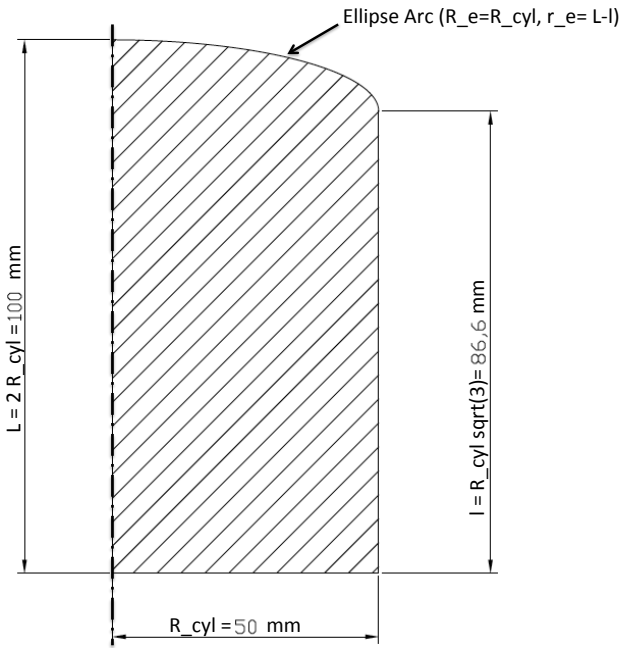

Figure 2. Geometry and dimensions of the "Iso-Q" specimen (in mm).

Table 2. Summary of the environment properties. Please use linear interpolation during the 0.1s heating and cooling periods (linear ramping).

time (s)	$\rho_e u_e C_h(0)$ (kg· m^{-2}· s^{-1})	h_e (J· kg^{-1})	$p_w(0,t)$ (Pa)	$p_w(11.17,t)$ (Pa)
0	$0.1 \cdot 10^{-2}$	0	405.3	405.3
0.1	0.1	$2.5 \cdot 10^7$	10132.5	405.3
40	0.1	$2.5 \cdot 10^7$	10132.5	405.3
40.1	$0.1 \cdot 10^{-2}$	0	405.3	405.3
120	$0.1 \cdot 10^{-2}$	0	405.3	405.3

- Heat and mass transfer assumptions in the boundary layer: $Pr = Le = 1$
- Re-radiation is active during the entire analysis [$q_r = \epsilon\sigma(T_w^4 - T_\infty^4)$]. Due to the convex shape of the test-specimens, a view factor of 1 is used. The infinity temperature is chosen to be $T_\infty = 300$ K .
- Use the wall enthalpy (h_w) and the B'_c table provided in the TACOT_3.0.xls file for code comparison.

The heat transfer coefficient and pressure profiles over the ellipsoid geometry have been estimated using a non-equilibrium aerothermodynamic hypersonic CFD code.[10] The free stream conditions used in this calculation are for air at a temperature of 225 K, at a density of 2.3×10^{-3} kg/m^3, traveling at 7000 m/s. A super-catalytic wall is used, at a temperature of 225 K.

For this test-case we will thus apply the heat-flux and pressure profile defined in Figure 3, where we pre-multiply $\rho_e u_e C_h(0)$ with the $q_w/q_w(0)$ values in Table 3. For the pressure it is slightly more complicated. At time $t = 0$ the pressure profile on the outer surface will be uniform ($p_w = 405.3$ Pa). During 0.1 seconds the pressure is increased (decreased for $5.18 \leq s \leq 7.07$) to $10132.5 \times p_w/p_w(0)$, using the pressure profile of Table 3. This pressure profile will be held constant until $t = 40.$ seconds. After this period, the surface pressure will be linearly reduced (during 0.1 seconds) to the initial uniform pressure of 405.3 Pa. At the stagnation point and the base this results in the time variation $p_w(s,t)$ given in Table 2.

We will use the TACOT wall enthalpy h_w and ablation rate B'_c values, obtained for different pressure values p_w between 0.001 and 1.0 atm. The back-side of the support structure is considered to be an adiabatic and impermeable wall.

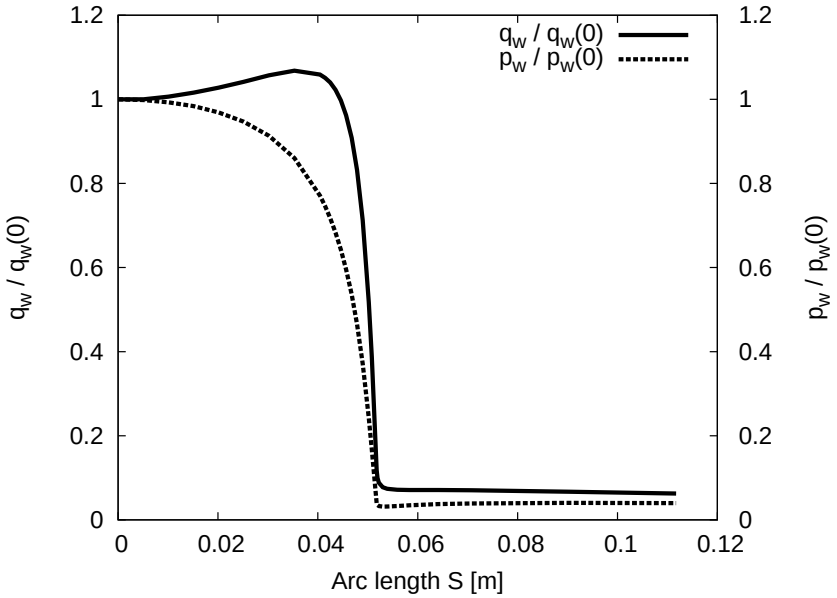

Figure 3. Heat flux and pressure distributions for the "Iso-Q" specimen.

Table 3. Distribution of the $q_w/q_w(0)$ values as a function of the Y- and Z-coordinate (plotted in Figure 3). In computations, please let vary the heat transfer coefficient (Ch), but not the edge enthalpy.

s (cm)	Y (cm)	Z (cm)	$q_w/q_w(0)$	$p_w/p_w(0)$	s (cm)	Y (cm)	Z (cm)	$q_w/q_w(0)$	$p_w/p_w(0)$
0.00	0.000	0.000	1.000	1.000	4.78	4.701	-0.884	0.833	0.466
0.51	0.507	-0.007	1.000	0.998	4.90	4.802	-0.967	0.712	0.371
1.01	1.008	-0.028	1.006	0.993	5.02	4.903	-1.078	0.518	0.243
1.51	1.509	-0.062	1.016	0.984	5.08	4.949	-1.149	0.388	0.167
2.01	2.008	-0.113	1.028	0.969	5.18	5.000	-1.348	0.118	0.039
2.51	2.505	-0.180	1.042	0.947	5.20	5.000	-1.411	0.100	0.035
3.02	3.009	-0.270	1.057	0.913	5.22	5.000	-1.505	0.088	0.033
3.53	3.508	-0.385	1.068	0.860	5.30	5.000	-1.757	0.078	0.031
4.04	4.007	-0.538	1.059	0.771	5.39	5.000	-2.009	0.074	0.032
4.15	4.105	-0.575	1.051	0.746	5.59	5.000	-2.497	0.071	0.033
4.25	4.202	-0.614	1.040	0.718	5.83	5.000	-3.001	0.071	0.035
4.35	4.304	-0.658	1.023	0.683	6.41	5.000	-4.009	0.071	0.038
4.46	4.405	-0.706	0.998	0.643	7.07	5.000	-5.001	0.070	0.039
4.57	4.503	-0.757	0.962	0.596	9.02	5.000	-7.504	0.067	0.040
4.68	4.604	-0.817	0.909	0.536	11.17	5.000	-9.992	0.063	0.040

IV. Test-case definitions

A total of four test-cases are defined, each one with an increasing complexity to go continuously from the series #2 test-cases to a general an-isotropic 3D test-case.

IV..1. Model with an isotropic material (Tests 3.0 and 3.1)

Two test-cases will be run with isotropic material properties, namely:

- 3.0: a 2D-axisymmetric model with an isotropic version of TACOT without ablation, as in test-case 2.1

(h_w is read from the $B_c^{'}$ table but $B_c^{'}$ is artificially taken equal to zero). This test is a non-physical test only meant to help code developers calibrate their codes before going into the model/code comparison, and may be skipped. Results for all type-2 codes are expected to be identical.

- 3.1: the same test but including ablation - and therefore, recession.

IV..2. Model with an orthotropic material (Test 3.2)

One of the goals of this test-series, is to compare the modeling capabilities of the different codes. One of the modeling capabilities, of practical interest, is to model orthotropic materials. For example PICA[6] is known to be orthotropic, where the through-the-thickness conductivity is lower that the isotropic conductivity, and the in-plane conductivity is higher than the isotropic conductivity. We therefore propose to use an orthotropic model, where the conductivities are defined via multiplication factors ($\alpha_1 = 1.0, \alpha_2 = 2.0$) for the isotropic conductivity of the TACOT model.

$$\begin{vmatrix} \lambda_{TTT} & 0 \\ 0 & \lambda_{IP} \end{vmatrix} = \begin{vmatrix} \alpha_1 & 0 \\ 0 & \alpha_2 \end{vmatrix} \lambda_{\text{isotropic}} \tag{1}$$

The through the thickness direction is aligned with the axis of axis-symmetry (Z-axis in Figure 1).

IV.A. A full 3D model with an orthotropic material (Test 3.3)

A final functionality that will be tested within series #3, is the full 3D modeling capabilities of the participating codes. The full 3D test will be a simple extension of the orthotropic material test of section IV..2. For this test, the through-the-thickness direction will form an angle $\alpha = 30^\circ$ (positive in the counter clock-wise direction) with the axis of axis-symmetry in the x=0 plane (see Figure 4). This configuration will lead to a

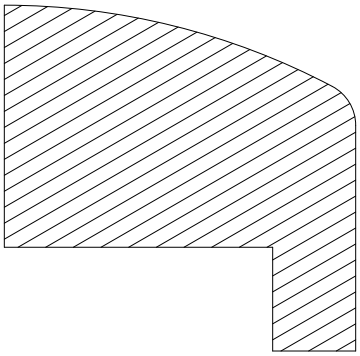

Figure 4. Visualization of the in-plane orientation.

full 3D problem with 3D heat and gas mass flow.

V. Material data

New thermochemical material properties have been generated for this test-case series. This was necessary because the pressure level of the test-case has been reduced, and the original data was only available at $p = 1.0$ atm. The material properties for this test-case series are provided [a] and explained in the spreadsheet TACOT_3.0.xls. The pyrolysis gas properties are generated as a function of temperature for three different values of the pressure ($p = 0.01, 0.1$ and 1.0 atm.). In Figure 5 the H_w and B_c' tables as a function of temperature is given for two values of the pressure (four values are calculated $p = 0.001, 0.01, 0.1$ and 1.0 atm.) and 25 values of B_g'.

The assumptions made, in order to get the new thermochemical values for TACOT, are the same as the ones made for version 2.2. Namely that an equilibrium calculation is performed, and that no condensed species are allowed to form in the mixture. The values are obtained with the TARGET[11] code

[a]Special thanks to Daniele Bianchi (E-mail: Daniele.Bianchi@uniroma1.it) for the generation of the updated TACOT thermochemistry data, using TARGET.

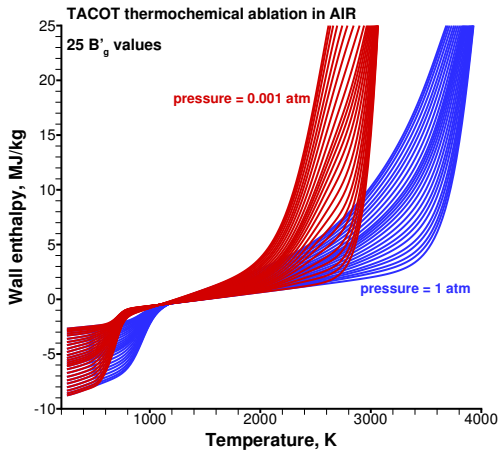

(a) H_w as a function of temperature and B'_g

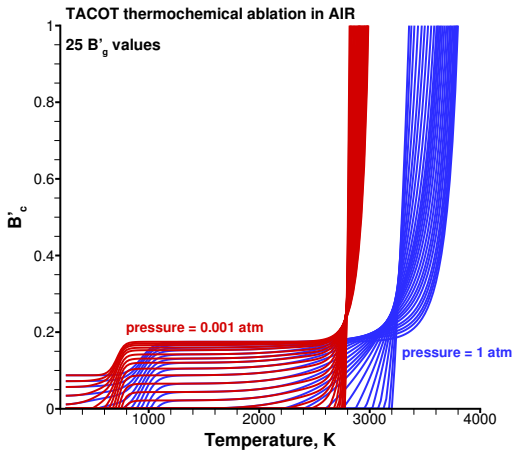

(b) B'_c as a function of temperature and B'_g

Figure 5. TACOT thermchemical ablation in AIR for different values of the pressure, using the TARGET[11] code.

(**T**hermochemical **A**blation **R**outine for the **G**eneration of **E**quilibrium **T**ables), which uses the CEA material data-base.

VI. Code output and comparison of the results

The results will be supplied in ASCII file format, which contain the following results (with an output frequency of 0.1 s):

- The temperature at the position of the stagnation point and of the 10 thermo-couples will be post-processed. The position of the thermo-couples are defined in Table 1 and Figure 1.
- For the same points (stagnation point and the thermo-couples) also the pressure and the density will be post-processed.

Output format desired:

time (s)	Tw (K)	T1 (K)	T2 (K)	T3 (K)	...	T8 (K)	T9 (K)	T10 (K)
0	3.000e2	3.000e2	3.000e2	3.000e2	3.000e2	3.000e2	3.000e2	3.000e2
0.1	9.651e2	3.225e2	3.000e2	3.000e2	3.000e2	3.000e2	3.000e2	3.000e2
0.2	1.076e3	3.956e2	3.039e2	3.000e2	3.000e2	3.000e2	3.000e2	3.000e2
etc.	...	...	...	...	...	...	...	...

Table 4. Output format for the temperature file: CodeName_Energy_TestCase_3-i.txt

time (s)	Pw (N/m2)	P1 (N/m2)	P2 (N/m2)	...	P10 (N/m2)
0	1.01325e4	1.01352e4	1.01352e4	1.01352e4	1.01352e4
0.1	1.01325e4	1.01352e4	1.01352e4	1.01352e4	1.01352e4
0.2	1.01325e4	1.01352e4	1.01352e4	1.01352e4	1.01352e4
etc.	...	...	...	...	...

Table 5. Output format for the pressure file: CodeName_Pressure_TestCase_3-i.txt

It is more convenient to generate separate result files for the four test cases of section III. We propose to use indices in the file names, where the i in the file names will refer to:

time (s)	rhow (kg/m3)	rho1 (kg/m3)	rho2 (kg/m3)	...	rho10 (kg/m3)
0	2.800e2	2.800e2	2.800e2	2.800e2	2.800e2
0.1	2.7900e2	2.800e2	2.800e2	2.800e2	2.800e2
0.2	2.7500e2	2.800e2	2.800e2	2.800e2	2.800e2
etc.	...	...	...	...	...

Table 6. Output format for the density file: CodeName_Density_TestCase_3-i.txt

- $i = 0$: Model with an isotropic material but without surface recession,
- $i = 1$: Model with an isotropic material,
- $i = 2$: Model with an orthotropic material,
- $i = 3$: A full 3D model with an orthotropic material.

VII. Preliminary results

In previous versions of the test-case, the pressure at the outer surface was held constant, due to an un-physical temperature drop at the beginning of the analysis. Because of the change in pressure values, the initial gas mass flow is smaller and so is the cooldown due to the negative value (equilibrium assumption of the pyrolysis gas) of the third term on the right hand side in the next equation:

$$q_i n_i = \rho_e u_e C_h \left[(h_e - h_w) + B'_c (h_c - h_w) + B'_g (h_g - h_w) \right] \tag{2}$$

Here the pressure distribution of Figure 3 is used. In order to start the transient analysis from an equilibrium solution the initial pressure distribution inside the test-specimen is calculated at time $t = 0$ seconds.

Besides the thermo-couple results, that need to be supplied for comparisons, additional results will be given in the annex of this report. These additional results will be helpful in identifying any problems that might arise when comparing the results of the different codes.

The results shown are generated with SAMCEF Amaryllis. Please do not give them more credit than they deserve and use them for sanity check rather than for comparison. In test-case 3.3 (numerical) oscillations were obtained in the temperature at the wall. The cause of these oscillations has not yet been identified. In all test-cases we see a (numerical) non-smooth pressure evolution during the cool-down phase. The cause for this behavior had not yet been identified.

Acknowledgments

We would like to thank you in advance for any comment that will help to improve the clarity of this document. Please send your comments to the authors.

References

[1]Lachaud, J., Martin, A., Cozmuta, I., and Laub, B., "Ablation Workshop Test Case - Version 1.1 - Feb. 2, 2011," Prepared for the 4^{th} Ablation Workshop (1-3 March 2011. Albequerque, New Mexico).

[2]Lachaud, J., Martin, A., van Eekelen, T., and Cozmuta, I., "Ablation test-case series #2 - Version 2.8 - Feb. 6, 2012," Prepared for the 5^{th} Ablation Workshop (28 February - 1 March 2012. Lexington, Kentucky).

[3]"Overview of Intercalibration Results," Thermal Performance Database Team, Oral presentation, 4^{th} Ablation Workshop (1-3 March 2011. Albequerque, New Mexico).

[4]Kendall, R. M., Bartlett, E. P., Rindal, R. A., and Moyer, C. B., "An Analysis of the Coupled Chemically Reacting Boundary Layer and Charring Ablator," Contractor report CR-1060, NASA, 1968.

[5]Empey, D. M., Skokova, K. A., Agrawal, P., Swanson, G. T., Prabhu, D. K., Peterson, K. H., and Venkatapathy, E., "Small Probe Reentry Investigation for TPS Engineering (SPRITE)," 8^{th} *International Planetary Probe Workshop*, IPPW-8, Portsmouth, Virginia, 2011.

[6]Milos, F. and Chen, Y.-K., "Two-Dimensional Ablation, Thermal Response, and Sizing Program for Pyrolyzing Ablators," *Journal of Spacecraft and Rockets*, Vol. 46, No. 6, December 2009, pp. 1089–1099.

[7]Agrawal, P., Ellerby, D. T., Switzer, M. R., and Squire, T. H., "Multidimensional Testing of Thermal Protection Materials in the Arcjet Test Facility," 10^{th} *AIAA/ASME Joint Thermophysics and Heat Transfer Conference*, No. AIAA 2010-4664, AIAA, 2010.

[8]Milos, F. and Chen, Y.-K., "Ablation and Thermal Response Property Model Validation for Phenolic Impregnated Carbon Ablator," *Journal of Spacecraft and Rockets*, Vol. 47, No. 5, September-October 2010, pp. 786–805.

[9]Dec, J. A., Laub, B., and Braun, R. D., "Two-Dimensional Finite Element Ablative Thermal Response Analysis of an Arcjet Stagnation Test," 42^{nd} *AIAA Thermophysics Conference*, No. AIAA 2011-3617, 27-30 June 2011.

[10]Martin, A., Scalabrin, L. C., and Boyd, I. D., "High performance modeling of an atmospheric re-entry vehicle," *Journal of Physics: Conference Series*, Vol. 341, 2012, pp. 1013.

[11]Bianchi, D., "A CEA-based Chemical Equilibrium Solver for Gas/Surface Thermochemistry and Thermochemical Tables Generation," *Centro Ricerca Aerospaziale Sapienza (CRAS),* Contract Reference no. CRAS-TTG-1001, Sapienza University of Rome, 2013.

Results of the test case series#3

2D and 3D finite element mesh

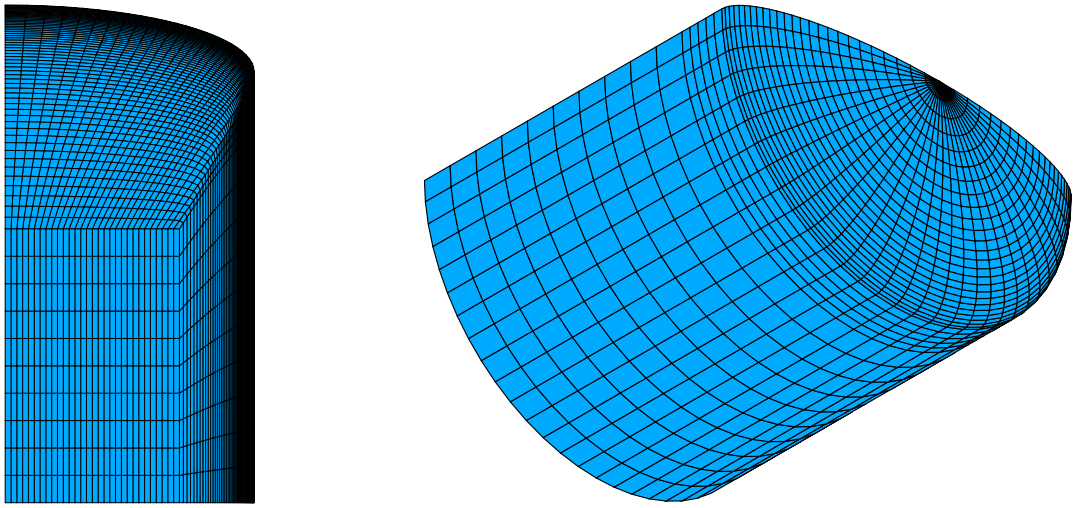

(a) 2D-mesh (b) 3D-mesh

Figure 6. Un-deformed finite element mesh.

Miscellaneous results for test-case 3.1, 3.2 and 3.3

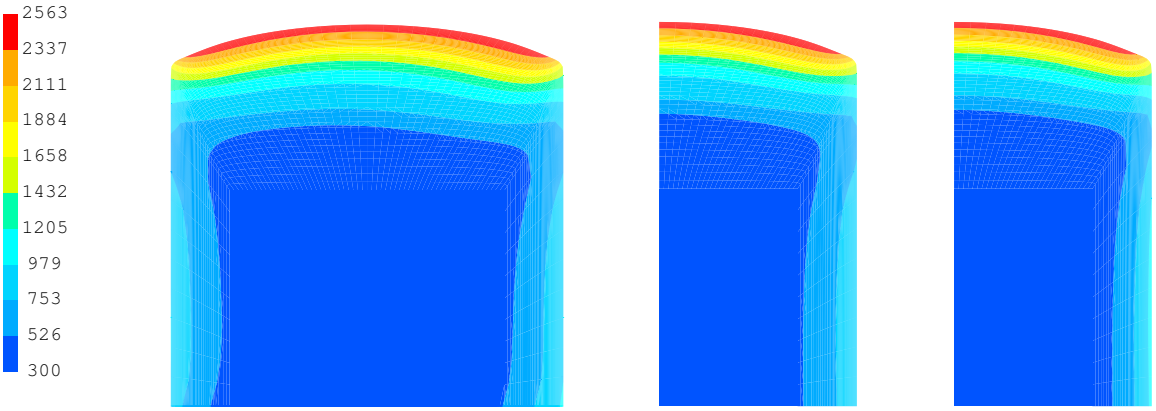

(a) Test-case 3.3 (b) Test-case 3.2 (c) Test-case 3.1

Figure 7. Temperature [K] distribution on a deformed structure at time t=39 seconds.

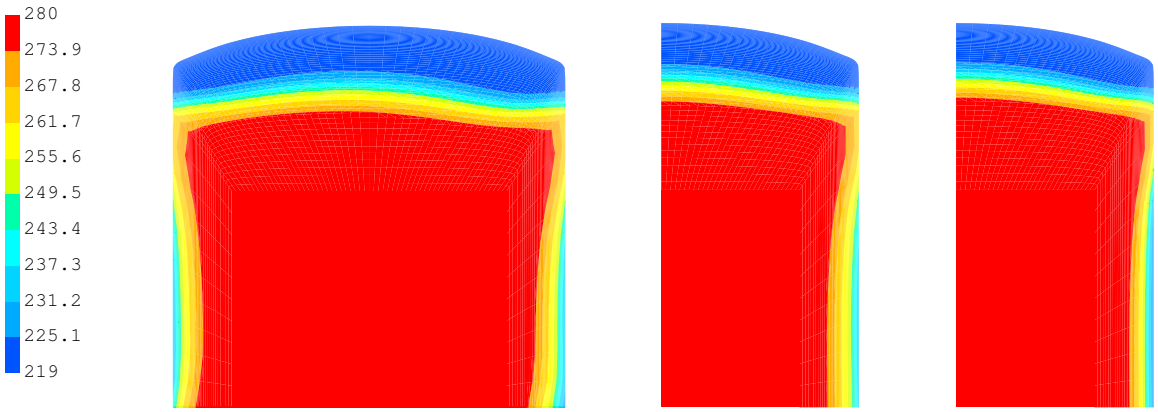

(a) Test-case 3.3 (b) Test-case 3.2 (c) Test-case 3.1

Figure 8. Density [kg/m^3] distribution on a deformed structure at time t=39 seconds.

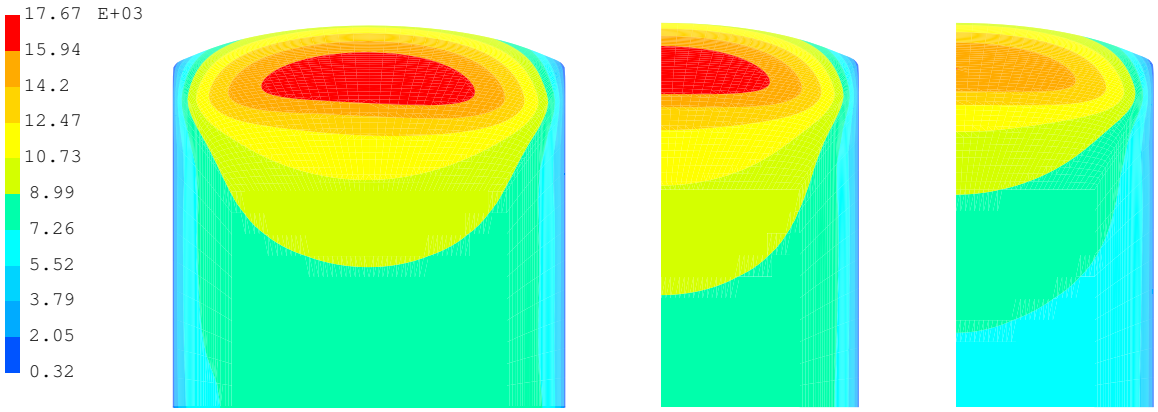

(a) Test-case 3.3 (b) Test-case 3.2 (c) Test-case 3.1

Figure 9. Pressure [N/m^2] distribution on a deformed structure at time t=39 seconds.

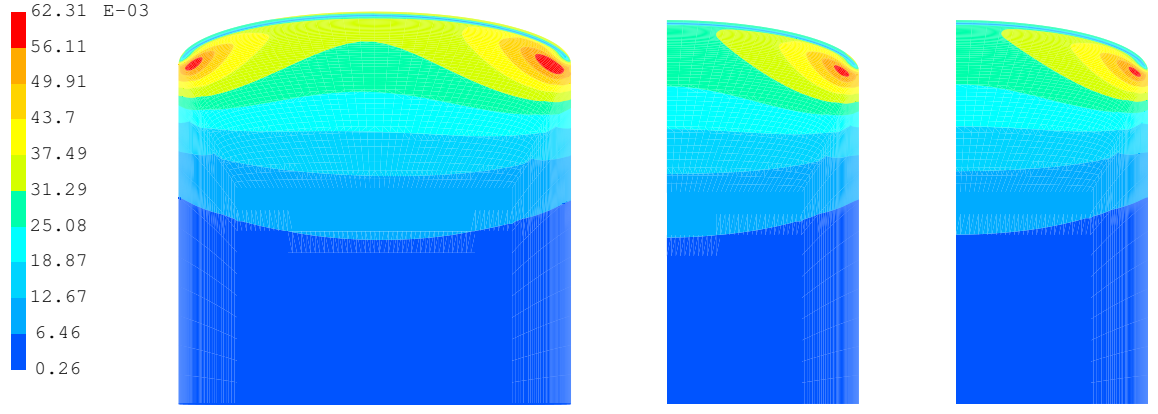

(a) Test-case 3.3 (b) Test-case 3.2 (c) Test-case 3.1

Figure 10. Gas mass flow [kg/(m^2.s)] distribution on a deformed structure at time t=0.8 seconds.

Surface results for test-case 3.0, 3.1, 3.2 and 3.3

The gas mass flow results given in the following figures is the modulus of the gas mass flow vector, i.e. this vector is not necessarily perpendicular to the outer surface.

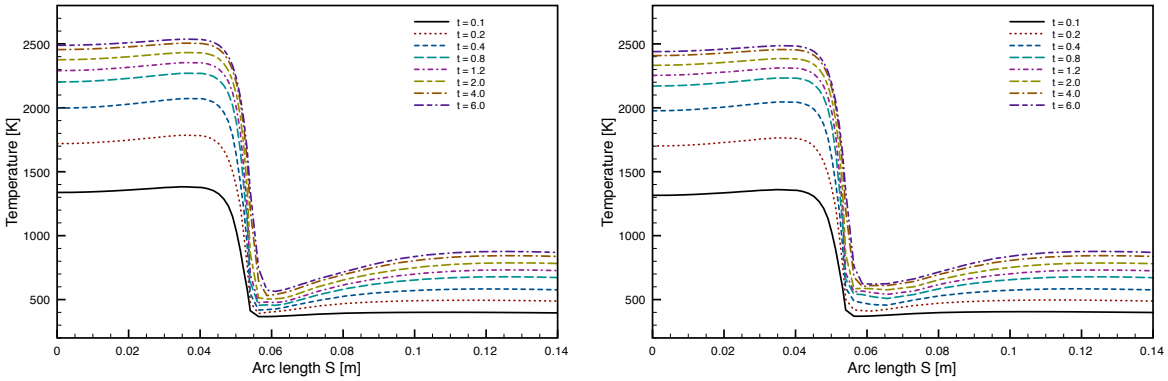

(a) Test-case 3.0 (b) Test-case 3.1

Figure 11. Temperature along the outer surface at different time instances.

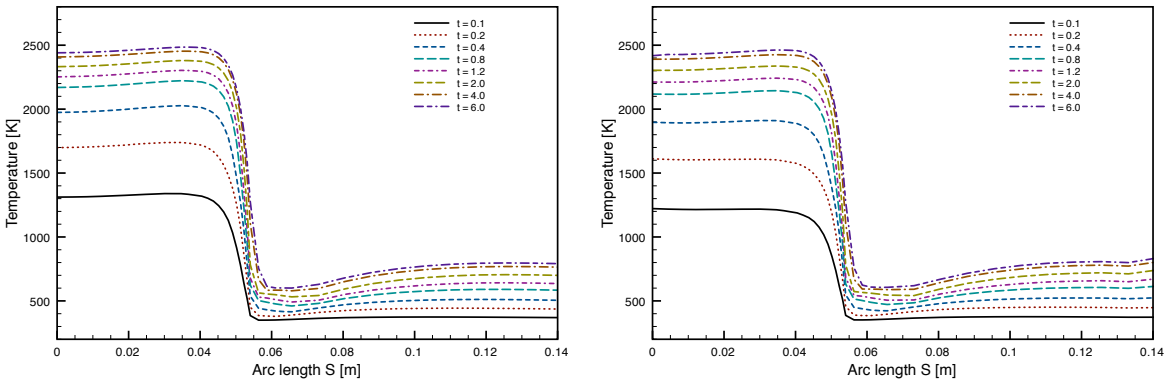

(a) Test-case 3.2 (b) Test-case 3.3

Figure 12. Temperature along the outer surface at different time instances.

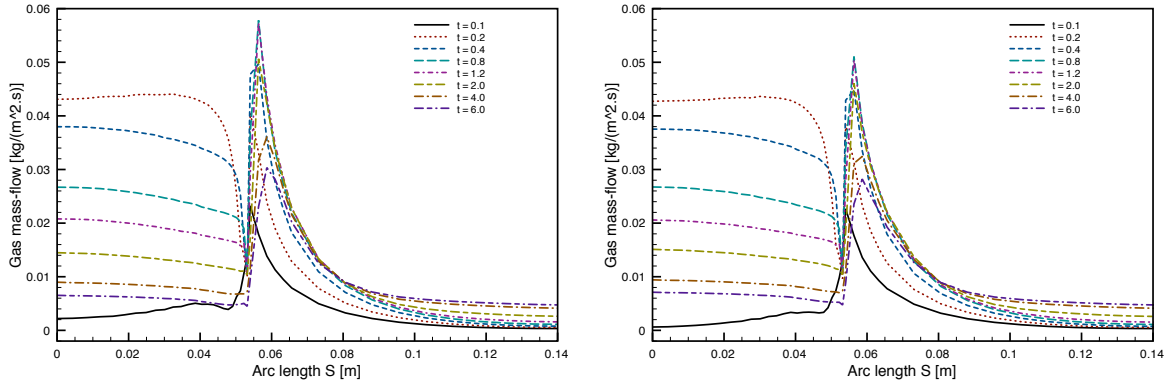

(a) Test-case 3.0 (b) Test-case 3.1

Figure 13. Modulus of the gas mass-flow along the outer surface at different time instances.

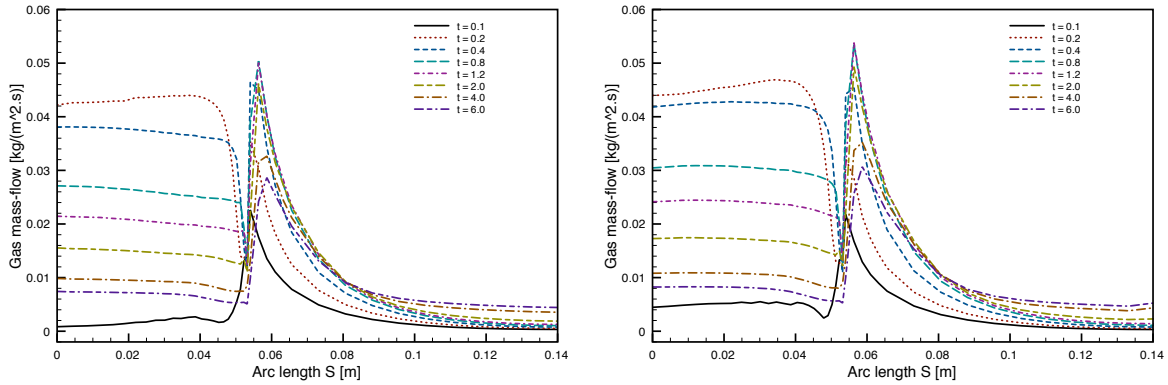

(a) Test-case 3.2 (b) Test-case 3.3

Figure 14. Modulus of the gas mass-flow along the outer surface at different time instances.

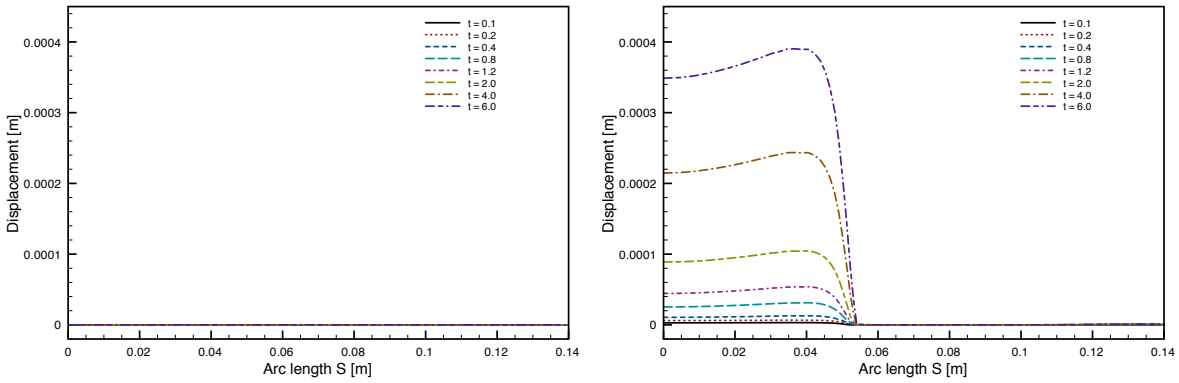

(a) Test-case 3.0 (b) Test-case 3.1

Figure 15. Modulus of the ablation deformation along the outer surface at different time instances.

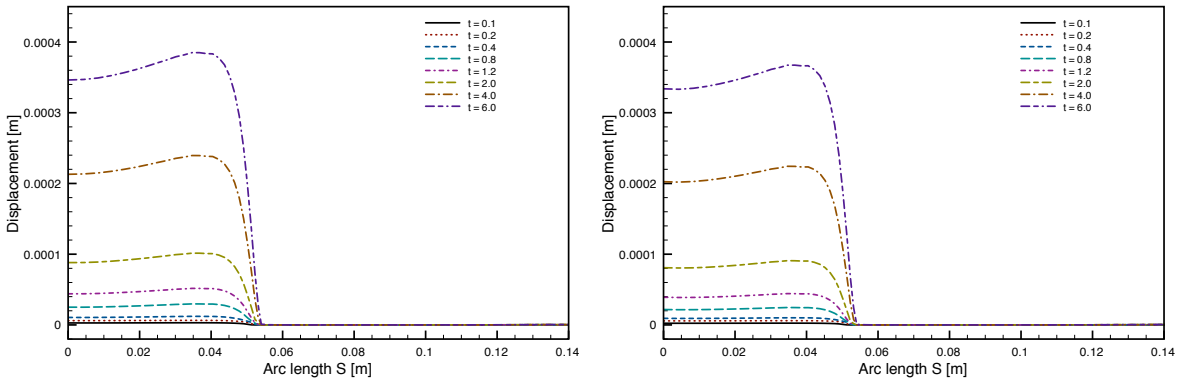

(a) Test-case 3.2 (b) Test-case 3.3

Figure 16. Modulus of the ablation deformation along the outer surface at different time instances.

Temperature curves for test-case 3.0, 3.1 and 3.2

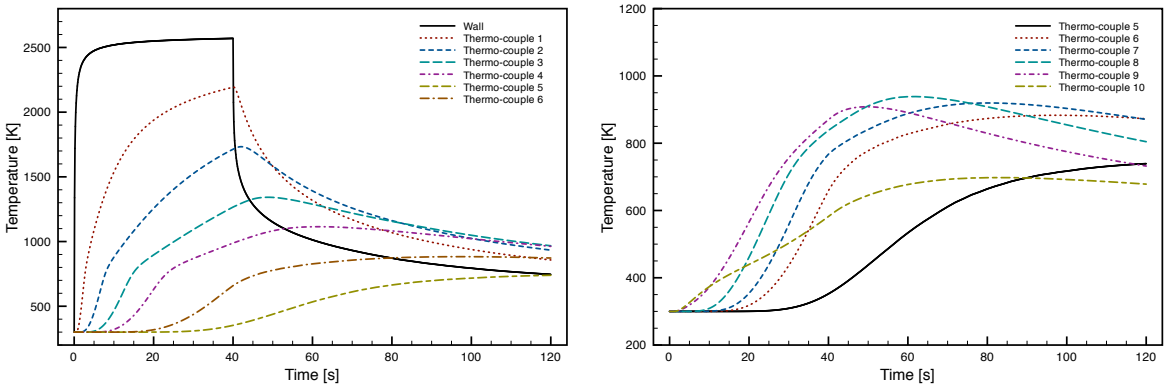

(a) thermo-couples 1 till 6 (b) thermo-couples 5 till 10

Figure 17. Temperature evolution of the wall and the thermo-couples for Test 3.0.

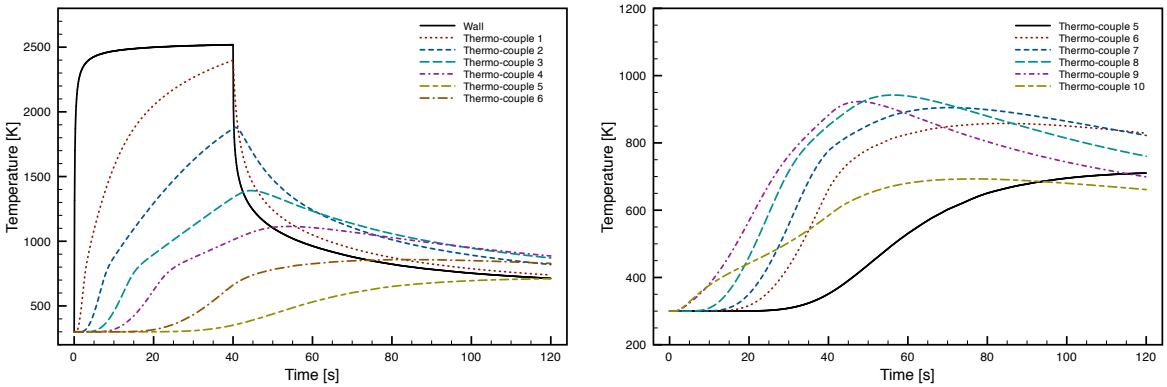

(a) thermo-couples 1 till 6 (b) thermo-couples 5 till 10

Figure 18. Temperature evolution of the wall and the thermo-couples for Test 3.1.

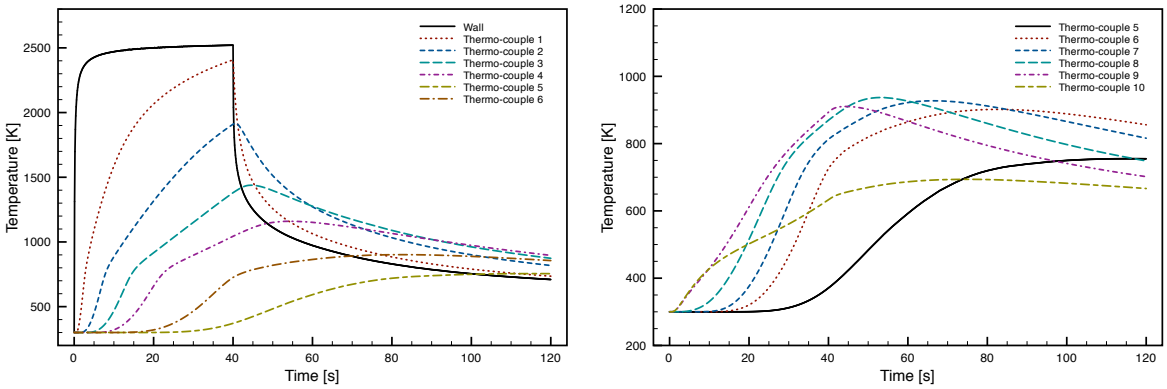

(a) thermo-couples 1 till 6 (b) thermo-couples 5 till 10

Figure 19. Temperature evolution of the wall and the thermo-couples for Test 3.2.

Pressure curves for test-case 3.0, 3.1 and 3.2

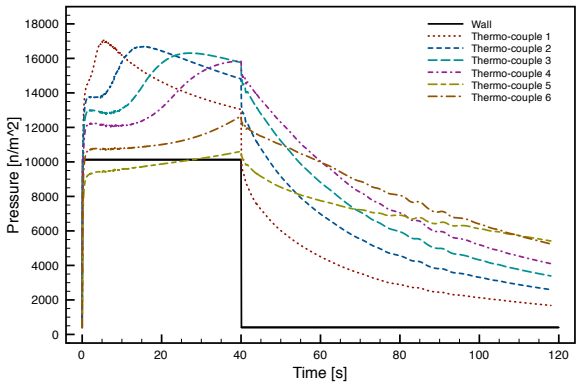

(a) thermo-couples 1 till 6

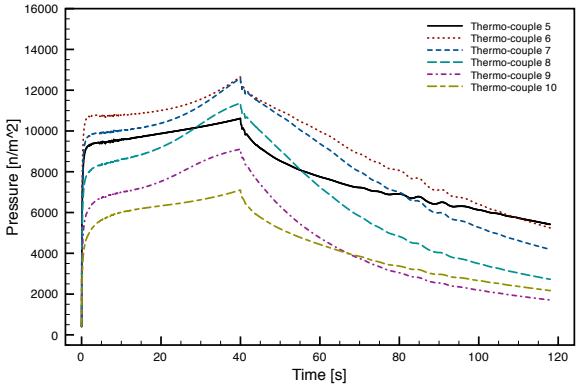

(b) thermo-couples 5 till 10

Figure 20. Pressure evolution of the wall and the thermo-couples for Test 3.0.

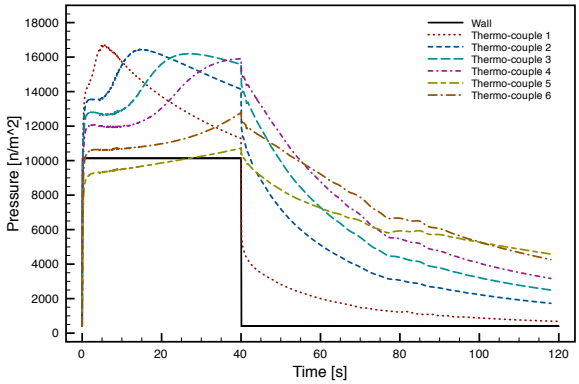

(a) thermo-couples 1 till 6

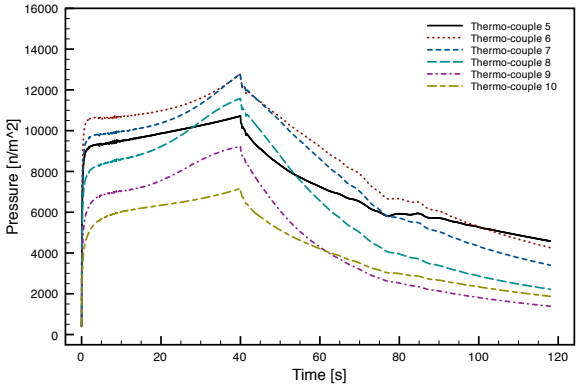

(b) thermo-couples 5 till 10

Figure 21. Pressure evolution of the wall and the thermo-couples for Test 3.1.

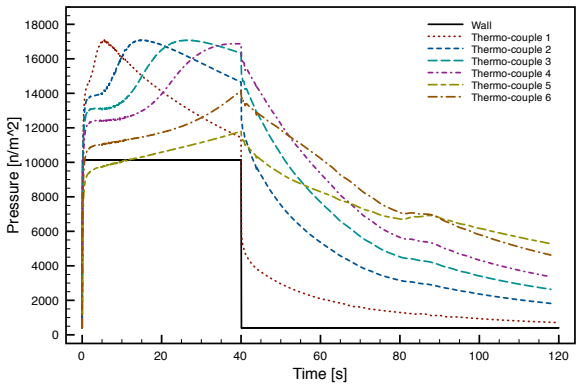

(a) thermo-couples 1 till 6

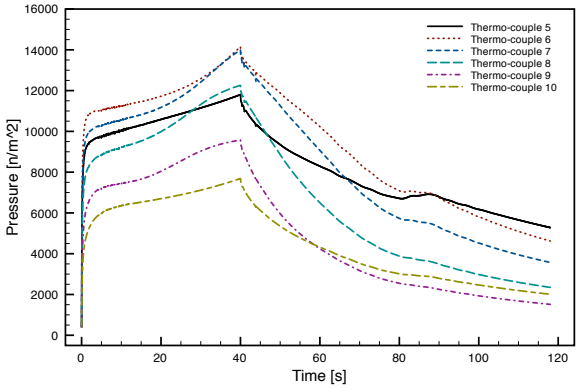

(b) thermo-couples 5 till 10

Figure 22. Pressure evolution of the wall and the thermo-couples for Test 3.2.

Density curves for test-case 3.0, 3.1 and 3.2

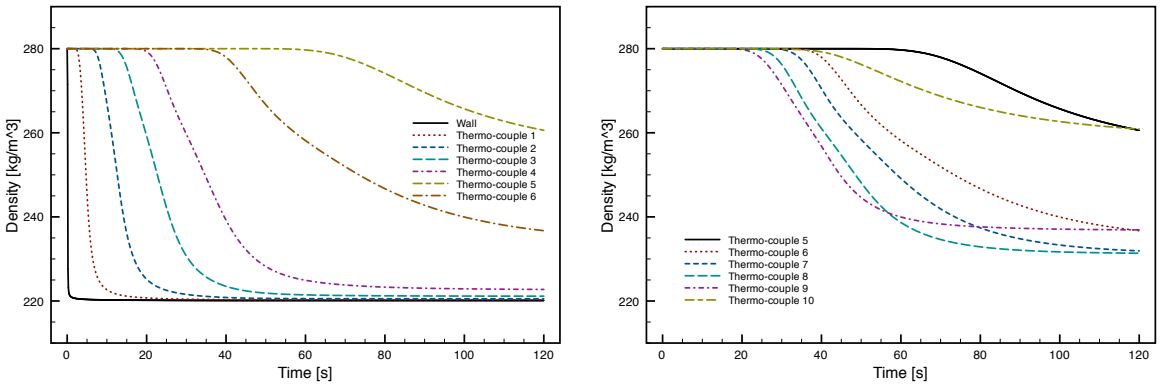

(a) thermo-couples 1 till 6 (b) thermo-couples 5 till 10

Figure 23. Density evolution of the wall and the thermo-couples for Test 3.0.

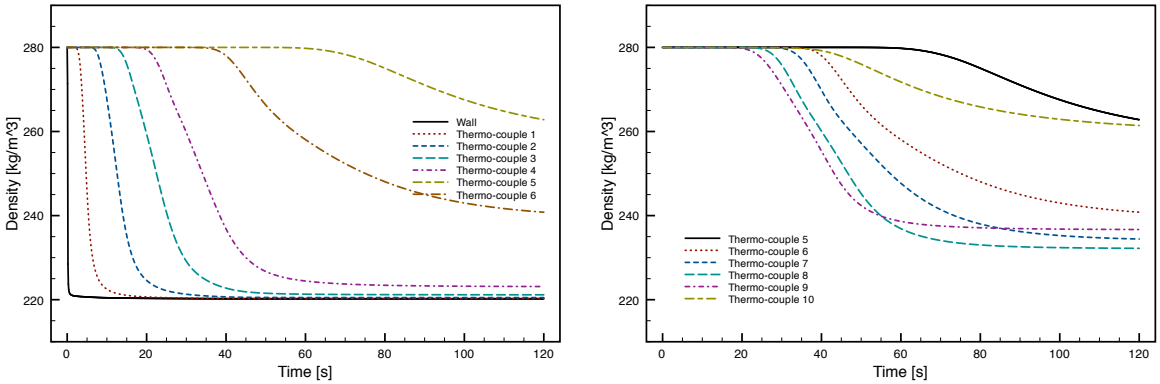

(a) thermo-couples 1 till 6 (b) thermo-couples 5 till 10

Figure 24. Density evolution of the wall and the thermo-couples for Test 3.1.

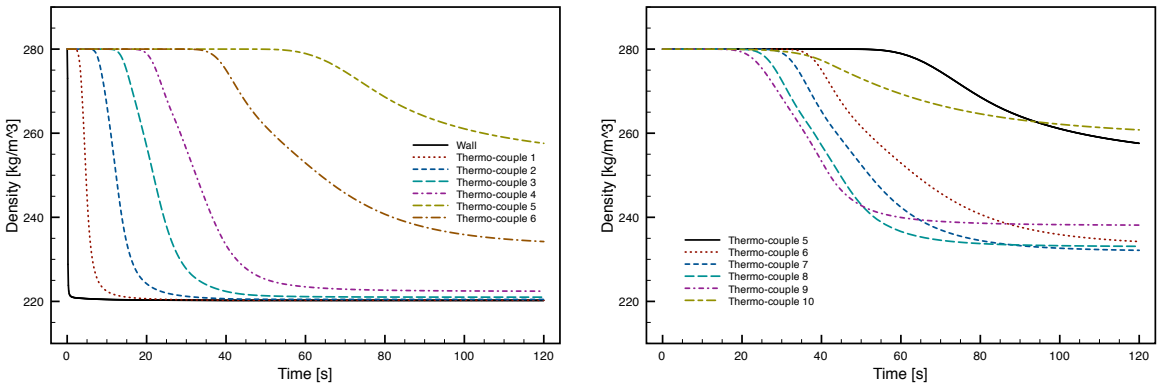

(a) thermo-couples 1 till 6 (b) thermo-couples 5 till 10

Figure 25. Density evolution of the wall and the thermo-couples for Test 3.2.

Comparison of temperature curves for test-case 3.2 and 3.3

In test-case 3.3 (numerical) oscillations were obtained in the temperature at the wall. The cause of these oscillations has not yet been identified.

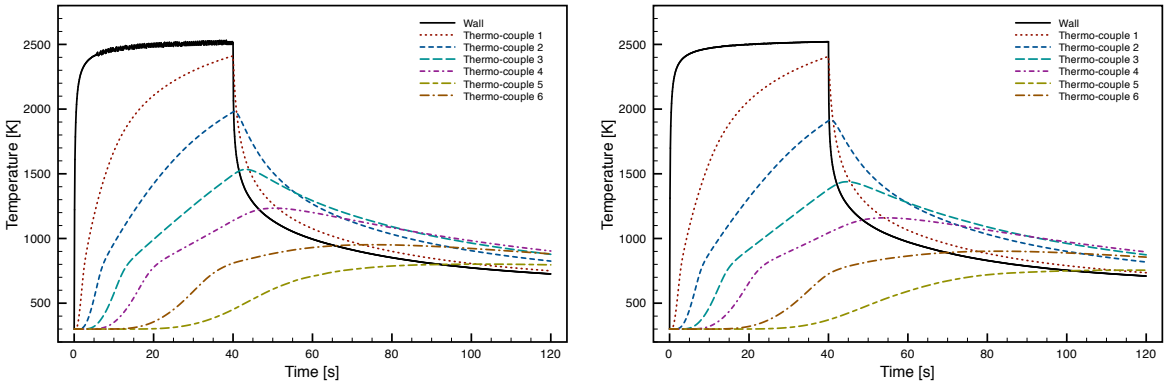

(a) Test 3.3 (b) Test 3.2

Figure 26. Temperature evolution of the wall end the thermo-couples 1 till 6.

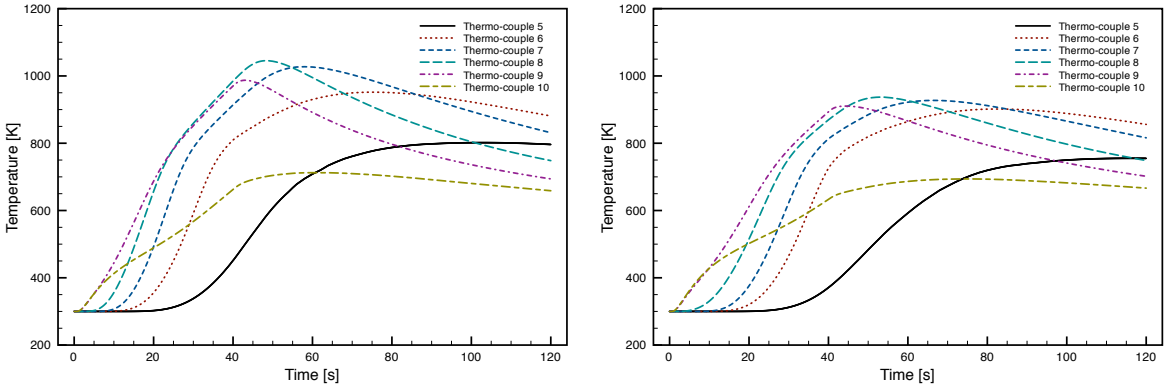

(a) Test 3.3 (b) Test 3.2

Figure 27. Temperature evolution of the thermo-couples 5 till 10.

Comparison of pressure curves for test-case 3.2 and 3.3

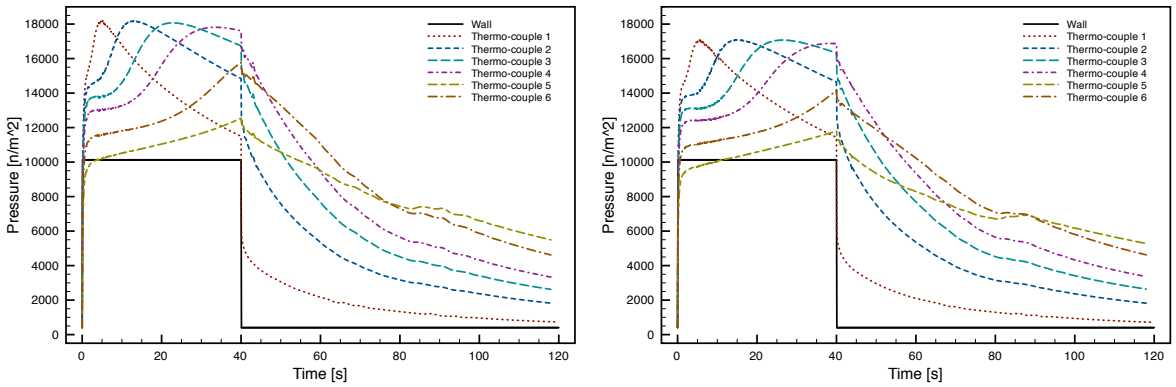

(a) Test 3.3 (b) Test 3.2

Figure 28. Pressure evolution of the wall and the thermo-couples 1 till 6.

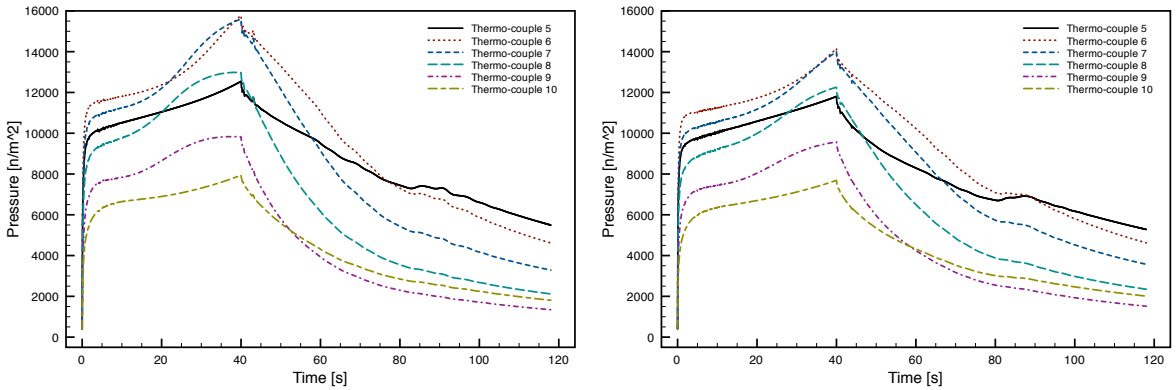

(a) Test 3.3 (b) Test 3.2

Figure 29. Pressure evolution of the thermo-couples 5 till 10.

Comparison of density curves for test-case 3.2 and 3.3

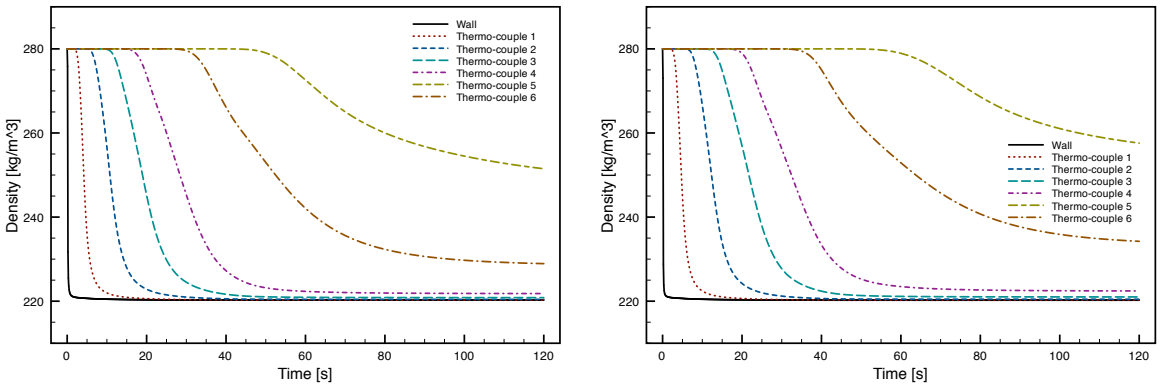

(a) Test 3.3 (b) Test 3.2

Figure 30. Density evolution of the wall and the thermo-couples 1 till 6.

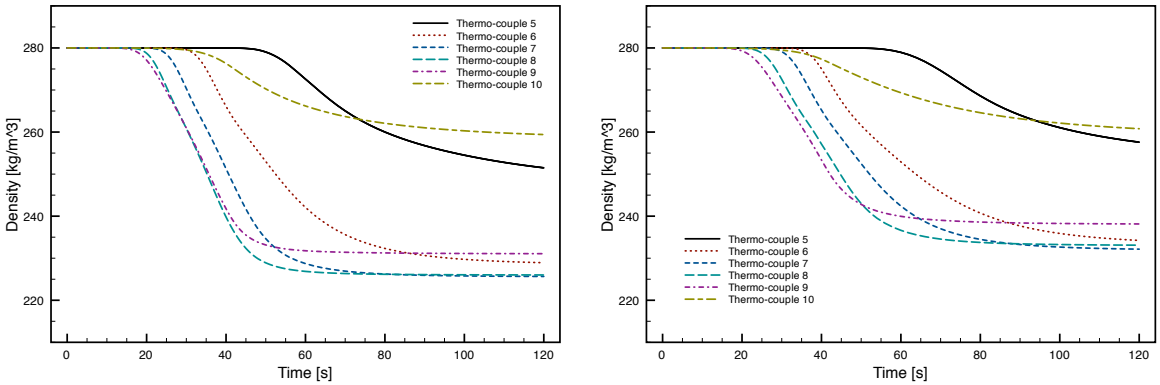

(a) Test 3.3 (b) Test 3.2

Figure 31. Density evolution of the thermo-couples 5 till 10.